

# Humidity-Induced Plasticization and Antiplasticization of Polyamide 6: A Positron Lifetime Study of the Local Free Volume

G. DLUBEK,<sup>1</sup> F. REDMANN,<sup>2</sup> R. KRAUSE-REHBERG<sup>2</sup>

<sup>1</sup> ITA Institut für innovative Technologien GmbH, Köthen, Aussenstelle Halle, Wiesenring 4, D-06120 Lieskau (bei Halle/S), Germany

<sup>2</sup> Martin-Luther-Universität Halle-Wittenberg, Fachbereich Physik, D-06099 Halle/S, Germany

Received 30 August 2000; accepted 2 August 2001

**ABSTRACT:** Polyamide 6 (PA6) was studied using positron annihilation lifetime spectroscopy (PALS). From the *ortho*-positronium lifetime  $\tau_3$  the size of local free volumes (holes) was estimated. In dry PA6 the mean hole volume  $v$  varied between  $70 \text{ \AA}^3$  and  $128 \text{ \AA}^3$  when the temperature increased from 25 to  $220^\circ\text{C}$ . From the comparison of the coefficient of thermal expansion of macroscopic volume with that of hole volume a number density of holes  $N_h$  of  $0.8 \text{ nm}^{-3}$  was estimated. The mean hole volume of PA6 exposed to atmospheres of different relative humidity (*RH*) was compared with the  $v(T)$  behavior of dry PA6. We propose a phenomenological model in which  $T_g$  and  $v_g$ , the glass transition temperature and the mean hole volume at  $T_g$ , are allowed to vary with *RH*. Assuming  $T_g(RH)$  as given in the literature, the  $v_g(RH)$  were estimated from our experiments. In the range  $0 < RH < 90\%$ , the  $v_g$  of the humid PA6 was always smaller than in the dry polymer, while near  $RH = 100\%$  both values became approximately identical. Two ranges of sorption behavior were observed. For small and medium *RH*,  $v_g$  decreases by up to  $19 \text{ \AA}^3$  for  $RH = 45\%$ , which corresponds to more than half of the volume of a water molecule. This behavior of  $v_g$  was interpreted as antiplasticization (loss of free volume) of the glassy polyamide. For larger *RH*,  $v_g$  increases again toward the value of dry PA6, indicating a plasticization (gain of free volume) behavior that compensates and finally nullifies the former antiplasticization. The behavior of the local free volume in moist PA6 corresponds well to the known variation of the specific volume. Our results deliver experimental evidence for the decrease in the unrelaxed free volume of the (glassy) water-PA6 mixture with respect to that of the dry glassy polymer. The results are also discussed in terms of a simple hole-filling model and of the hypothesis of firmly and loosely bound water molecules in polyamides. © 2002 John Wiley & Sons, Inc. *J Appl Polym Sci* 84: 244–255, 2002; DOI 10.1002/app.10319

**Key words:** polyamides; nylon; glass transition; solution properties

## INTRODUCTION

Amorphous polymers contain cavities or holes of atomic and molecular dimension that arise because of irregular molecular packing in the glassy

phase and segmental motion in the rubbery phase.<sup>1</sup> The sum of these holes is described as free volume, which may be defined as the volume of an amorphous polymer being in excess to a hypothetical occupied volume. The free volume affects many physical properties of polymers. The diffusion of small molecules (gases, organic, and inorganic liquids) in glassy polymers occurs through local free volumes.<sup>2</sup> The polyamides (nylons) form a group of polymers that can absorb up to approx-

Correspondence to: G. Dlubek (GDlubek@aol.com).

*Journal of Applied Polymer Science*, Vol. 84, 244–255 (2002)  
© 2002 John Wiley & Sons, Inc.

imately 10 wt % of water from the ambient atmosphere. The water modifies mechanical and dielectric properties of the polyamides.<sup>2-9</sup> Although water sorption has been investigated for more than 30 years, the mechanism of incorporation of water molecules into the polymer structure is still a matter of discussion.

The basis ideas of the mechanism of water sorption in polyamide 6 (PA6,  $[-\text{NH}-(\text{CH}_2)_5-\text{CO}-]_n$ ) were developed by Puffr and Sebenda,<sup>3</sup> who deduce a two-step model. In this model it is assumed that in PA6, three molecules of water are bound on two neighboring amide groups in an accessible region. The first molecules form a double hydrogen bond between the carbonyl groups. In this step a large amount of heat is evolved. Therefore, this water may be assessed as firmly (or tightly) bound water. The second and third water molecules join the already existing H bonds from the NH groups to other CO groups with a negligible thermal effect. Consequently, this water is denoted as loosely (or weakly) bound. This two-step model was later extended by Starkweather,<sup>4,5</sup> who considered a clustering of water molecules.

Water is sorbed mainly by the amorphous phase of polyamides, and causes the glass transition temperature to decrease.<sup>7,9</sup> This one would expect if the diluent had more free volume associated with it than that naturally occurring in the (dry) polymer. The specific volume of the moist polyamides, however, shows a negative departure from the rule of additivity.<sup>4,5</sup> This densification or loss in free volume appears to be in contradiction to the free volume concept of glass transition.<sup>1,10,11</sup> Several structural and phenomenological models are presented to understand this phenomenon denoted as antiplasticization.<sup>12-15</sup> Thus, it was argued that the behavior of the specific volume can be described phenomenologically assuming a decrease in the unrelaxed (free) volume of the water-polymer mixture with respect to that of the pure glassy polymer.<sup>12-15</sup>

In this work we investigate the free volume in PA6 using positron annihilation lifetime spectroscopy (PALS), a well-established and very sensitive technique for probing subnanometer-size local free volumes in amorphous polymers.<sup>16-20</sup> We compare the temperature dependence of the free volume in dry PA6 in the range between 25 and 220°C with changes in the free volume due to isothermal moisture sorption from ambient atmospheres of different relative humidities. From this comparison we hope to obtain information that will contribute to the understanding of the reasons and mechanism of

humidity induced antiplasticization. A few positron studies on moisture sorption in polyamides were published in the past,<sup>21-24</sup> most recently by Welander and Maurer<sup>23</sup> in 1991, and by some of the authors of this article<sup>24</sup> in 1998. To our best knowledge there is only one article, published in 1972 by Chuang et al.,<sup>21</sup> dealing with the temperature dependence of the free volume in PA6 in the limited temperature range from 25 to 100°C.

## EXPERIMENTAL

The samples investigated in this study were made from a commercial polyamide 6 (Ultramid B35W, BASF, Germany, the same material that we studied previously<sup>24</sup>). PA6 granulate was hot pressed to plates of 1.5 mm thickness and quenched from 220°C into water of room temperatures. Subsequently, the plates were annealed at 200°C for 3 h. From wide-angle X-ray scattering investigation a crystallinity of 22% was estimated. All positron lifetime measurements were carried out using a fast-fast coincidence PALS system<sup>25</sup> with a time resolution of 230 ps (full width at half maximum, FWHM, of a Gaussian resolution function) and a channel width of 50.12 ps. For each experiment, two identical samples were sandwiched around a  $4 \times 10^6$  Bq positron source (<sup>22</sup>Na), which was prepared by evaporating carrier-free <sup>22</sup>NaCl solution on an aluminum foil of 2 mg/cm<sup>2</sup> mass thickness. The time resolution of the apparatus and the source components (165 ps/4.0%—Al foil, 360 ps/3.7%—NaCl salt, 2000 ps/0.4%—surface effects) were estimated from measurement of a reference sample made of p-type Si ( $\tau = 219$  ps).

Depending on the type of experiment the measurement of a spectrum lasted 2, 4, or 16 h, resulting in a total number of annihilation events within a spectrum of 4, 8, or 32 *M*. For temperature-dependent measurements the sample-source sandwich was placed in a vacuum chamber allowing a vacuum of  $5 \times 10^{-4}$  Pa. Before starting the measurements, the sample was dried in vacuum for 36 h. For heating the samples a small resistivity heater was used, the temperature was controlled with a Eurotherm controller with an accuracy of  $\pm 1^\circ\text{C}$ . For the experiments on moist PA6 the sample was first exposed for 4 days to an atmosphere of defined relative humidity (*RH*) followed by 12 2-h lifetime measurements in laboratory air (*RH*  $\approx$  40%). To maintain a precisely controlled relative humidity over long periods of

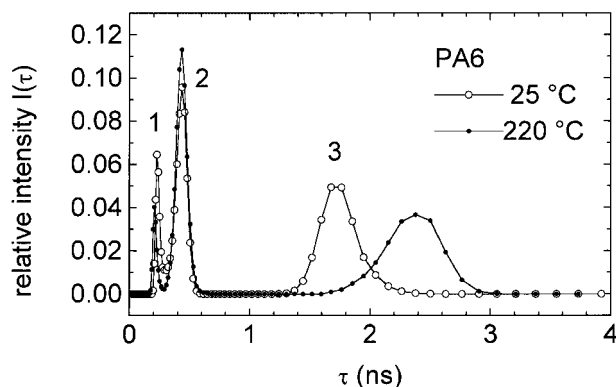


**Figure 1** Positron lifetime intensity distribution  $I(\tau)$  derived from lifetime spectra (32  $M$  total count) using the routine MELT. The experiments on PA6 were performed in a vacuum at 25 and 220°C.

time, saturated salt solutions were used.<sup>26,27</sup> The atmosphere above these solutions had relative humidities  $RH$  of 11% (LiCl), 32% (MgCl<sub>2</sub>), 45% (K<sub>2</sub>CO<sub>3</sub>), 55% (NaBr), 75% (NaCl), and 90% (BaCl<sub>2</sub>), 100% (pure water).

For the decomposition of the lifetime spectra  $s(t)$  we used the conventional analysis in terms of a weighted sum of discrete exponentials,<sup>25</sup>

$$s(t) = \sum (I_i/\tau_i) \exp(-t/\tau_i) \quad \sum I_i = 1. \quad (1)$$

where  $\tau_i$  denotes the mean (characteristic) lifetime of the positron/Ps state  $i$ , while  $I_i$  is the relative intensity of the corresponding lifetime component. In this type of analysis the number of exponentials has to be assumed. The parameters are obtained from a nonlinear least-squares fitting of  $s(t)$  to the experimental spectra using the routine LIFSPECFIT.<sup>28</sup> This analysis was complemented applying the program MELT (Maximum Entropy for Lifetime Analysis<sup>29</sup>), which assumes a continuous lifetime distribution without the necessity of assuming the number of components. Instead of discrete components ( $\delta$ -functions), the routine MELT delivers a distribution consisting of Gaussian-like peaks. The characteristic lifetime  $\tau_i$  and its intensity  $I_i$  are calculated as mass center and relative area of the corresponding peak.

## RESULTS AND DISCUSSION

### The Nature of the Positron Lifetime Spectra

In Figure 1 the positron lifetime intensity distribution  $I(\tau)$  estimated from the 32  $M$  count lifetime

spectrum using the routine MELT is shown as an example for the temperatures of 25 and 220°C. In molecular materials, such as polymers, a fraction of the injected positrons form and annihilate from a bound state called positronium (Ps).<sup>25</sup> The Ps appears either as a *para*-positronium (*p*-Ps, singlet *spin* state) or as an *ortho*-positronium (*o*-Ps, triplet *spin* state) with a relative formation probability of 1:3. Three peaks (lifetime components) appear in the distribution, conventionally attributed to annihilation of *p*-Ps (peak 1), free (not Ps) positrons (peak 2), and *o*-Ps (peak 3, Fig. 1). In vacuum, an *o*-Ps has a relatively long lifetime of 142 ns. In fact, during collisions with molecules, the positron of the Ps may annihilate with an electron other than its bound partner and with opposite spin (pick-off annihilation). The result is a sharply reduced *o*-Ps lifetime depending on the frequency of collisions. In the presence of a sufficient concentration of small holes (local free volumes) in the sample, the Ps density is largely confined within these open volumes and their size/volume is reflected in the *o*-Ps pick-off lifetimes, lying in the low ns-range.<sup>16–20</sup> The shift of the *o*-Ps peak to higher lifetimes (Fig. 1) mirrors the increase in the average size of local free volumes when increasing the temperature from 25 to 220°C. The broadening of the *o*-Ps peak is conventionally attributed to a size and shape distribution of holes.<sup>18</sup>

From the lifetime distribution at 25°C the mass centers of a peak,  $\tau_i$ , and relative areas below a peak,  $I_i$ , of 217 ps/31.6%, 422 ps/47.3%, and 1715 ps/21.1% were estimated. Similar results were obtained from an unconstrained three discrete term fit to the lifetime spectrum. We did not find clear indications for a second *o*-Ps lifetime that might be attributed to *o*-Ps annihilation in PA6 crystals. It is well known that the Ps formation in polymer crystals is, if not zero,<sup>30,31</sup> distinctly smaller than in the amorphous phase<sup>32,33</sup> (see also the extensive discussion in a previous article<sup>24</sup> about the situation in polyamides). Following the literature,<sup>21–23</sup> we therefore ignore a possible contribution of crystals to the lifetime spectra in PA6.

The ratio  $I_1/I_3 = 31.6/21.2 = 1.49$  is distinctly larger than the theoretical expectation of  $I_{p\text{-Ps}}/I_{o\text{-Ps}} = 1/3$ , the ratio of *p*-Ps and *o*-Ps formation probabilities.<sup>25</sup> Also, the lifetime  $\tau_1 = 217$  ps appears rather large compared with the lifetime of *p*-Ps in vacuum (125 ps). The overestimation of  $I_1$  in the lifetime analysis is a well-known observation. Recently, it was found that this may be

understood as an artifact of the spectrum analysis caused by a positron ( $e^+$ ) lifetime distribution.<sup>34</sup> Analogous to the *o*-Ps lifetimes their distribution in polymers is well accepted, the  $e^+$  lifetimes may also be distributed due to the annihilation of positrons from local free volumes or other empty spaces that have a distribution in sizes and shapes. Unfortunately, the lifetime distributions analyzed with the routine MELT (and CONTIN) also show the artifacts mentioned above, although reduced when comparing with results of the unconstrained discrete term analysis. As discussed in detail in previous article,<sup>34</sup> this difficulty may be overcome using a constrained discrete term fit to lifetime spectra in which the intensity ratio  $I_1/I_3$  is fixed to the theoretical value of 1/3. This constraint involves the assumption that pick-off annihilation is the only *o*-Ps quenching process. Doing this, we obtained for the lifetime parameters of the 25°C spectrum  $\tau_i/I_i = 128 \text{ ps}/7.8\%$ ,  $346 \text{ ps}/68.5\%$ , and  $1693 \text{ ps}/23.7\%$ . In the following we will discuss lifetime results obtained via this type of analysis.

From the *o*-Ps pick-off lifetime  $\tau_3$  the mean size of local free volumes (holes) in which Ps annihilates may be estimated. A simple model incorporating quantum mechanical and empirical arguments provides an analytic expression relating the hole (assumed spherical) radius ( $r$ ) to the observed *o*-Ps pick-off lifetime,<sup>16–18</sup>

$$\tau_3 = \tau_{p0} = 0.5 \text{ ns} \left[ 1 - \frac{r}{r + \delta r} + \frac{1}{2\pi} \sin \left( \frac{2\pi r}{r + \delta r} \right) \right]^{-1}. \quad (2)$$

The premultiplicative factor of 0.5 ns is the spin-averaged Ps annihilation lifetime that is also observed in densely packed molecular crystals.  $\delta r$  represents the extent of the penetration of the Ps wave function into the walls of the hole that is modeled by a square well potential of infinite depth and radius  $r$ . A widely used value of  $\delta r = 0.166 \text{ nm}$  is obtained by fitting eq. (2) to observed *o*-Ps lifetime of known mean hole radii in porous materials.<sup>16,17</sup> From the *o*-Ps lifetime of  $\tau_3 = 1693 \pm 5 \text{ ps}$ , estimated from the 25°C spectrum a mean hole radius of  $r = 2.55 \pm 0.02 \text{ \AA}$  and a mean hole volume of  $v = 70 \pm 2 \text{ \AA}^3$  follow. The lifetime of  $\tau_3 = 2302 \pm 5 \text{ ps}$  observed at 220°C corresponds to  $r = 3.17 \pm 0.2 \text{ \AA}$  and  $v = 128 \pm 2 \text{ \AA}^3$ .

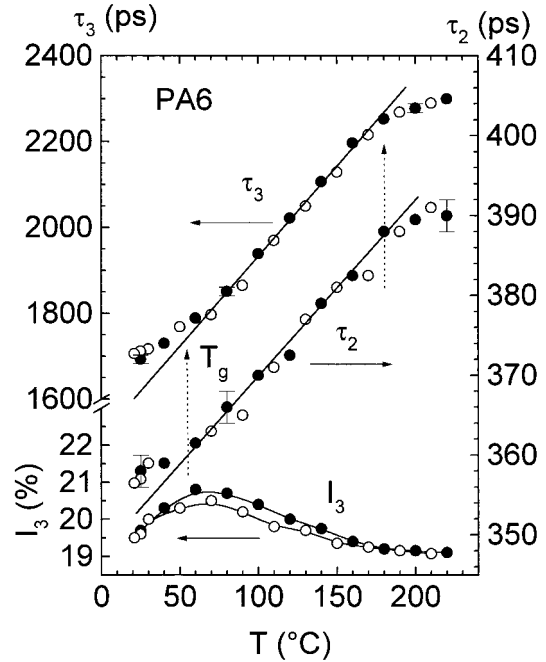


**Figure 2** The *o*-Ps lifetime  $\tau_3$ ,  $e^+$  lifetime  $\tau_2$ , and intensity  $I_3$  in PA6 as a function of the temperature of measurement  $T$ . Filled symbols: increasing temperatures, empty symbols: decreasing temperatures.

### The Temperature Dependence of the Local Free Volume

For temperature-dependent measurements the PA6 sample was placed in the vacuum chamber, and after 36 h of pumping the lifetime measurements were started. The results of this experiment ( $\tau_3$ ,  $\tau_2$ , and  $I_3$ ) are shown in Figure 2. The lifetime spectra were measured during increasing and decreasing temperatures. Each of the shown parameters represents the average of two 4 h (each with 8  $M$  total count) measurements. The data were well reproducible within the statistical errors of the experiment. As can be observed in Figure 2,  $\tau_3$  increases from 1690 ps at 25°C to a value of 2300 ps at 220°C, which indicates an increasing mean local free volume. The *o*-Ps lifetime  $\tau_3$  does not show any hysteresis. The *o*-Ps intensity  $I_3$  shows a small temperature variation and some hysteresis. Because  $I_3$  may be affected by a large variety of processes,<sup>25</sup> we will not discuss its behavior in the current work.

The  $e^+$  lifetime  $\tau_2$  shows a similar behavior to  $\tau_3$  increasing from 358 ps at 25°C to 390 ps at 220°C. The temperature variation of  $\tau_2$  may be considered as evidence that positrons ( $e^+$ , not Ps) annihilate in local free volumes of amorphous

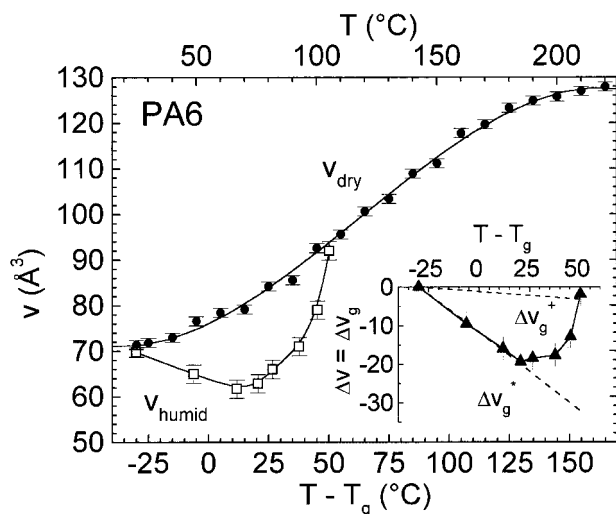


**Figure 3** The variation in the hole volume in dry PA6,  $v_{\text{dry}}$ , with varying temperatures and in humid PA6,  $v_{\text{humid}}$ , for different moisture sorptions. The hole volumes are plotted vs.  $T - T_g$  where for the dry polymer  $T_g = 54^\circ\text{C}$  and  $T$  is the varying temperature of measurement (upper scale). In the humid polymer  $T_g$  is a function of relative humidity  $RH$  of the atmosphere to which the sample was exposed [see text and eq. (5)] and  $T = 25^\circ\text{C}$  is the temperature of measurement. The subfigure shows the difference in the local free volume of the humid and dry polyamide at the glass transition  $\Delta v = \Delta v_g = v_{\text{humid},g} - v_{\text{dry},g}$ .  $\Delta^+v_g$  and  $\Delta^-v_g$  denote model calculations for maximum and no antiplasticization (i.e., loss of free volume) of the glassy PA6–water mixture (see text).

polymers and their lifetime responds to the mean hole size. As mentioned above, this has been assumed in previous works,<sup>34</sup> but due to the statistical scatter in  $\tau_2$ , this effect was rarely observed.<sup>18,35</sup>

If a straight line is fitted to the  $\tau_3$  and  $\tau_2$  data, a deviation from this line is observed for temperatures below  $55^\circ\text{C}$  and above  $180^\circ\text{C}$ . The deviation at lower temperatures may be related to the glass transition of PA6 ( $T_g = 54^\circ\text{C}$ ),<sup>9</sup> the possible origin of the higher deviation point we will discuss later. The lifetime parameters derived from an unconstrained three discrete term analysis show the same behavior as the parameters plotted in Figure 2, except the larger statistical scatter, especially in  $\tau_2$  and  $I_3$ .

In Figure 3 the mean hole volume of the dry PA6,  $v = v_{\text{dry}}$ , estimated via eq. (2), is plotted together with the hole volume of the humid polymer  $v_{\text{humid}}$  as a function of  $T - T_g$ , where  $T$  is the temperature of measurement. The  $T$  for the dry polymer is shown in the top scale of the Figure. In

the temperature range between  $T = 25$  and  $220^\circ\text{C}$  the hole volume in the dry PA6,  $v_{\text{dry}}$ , varies between 70 and  $128 \text{ \AA}^3$ . Below  $T_g = 54^\circ\text{C}$  the polymer is in the glassy state. The *o*-Ps detects pre-existing static holes. With increasing temperature the local free volumes show a weak thermal expansion. In the rubbery phase,  $T > T_g$ , the molecular and segmental motion increases and the free-volume holes obtain a more dynamic character. The mean hole size increases distinctly with increasing temperature.

As stated previously, the increase of the *o*-Ps lifetime  $\tau_3$  with temperature slows down above  $180^\circ\text{C}$  and tends to level off. Such a behavior has already been observed previously,<sup>18,36</sup> its nature, however, is not well understood. Often it is attributed to the formation of Ps bubbles in the liquid-like state of a polymer, i.e., due to the high mobility of polymer segments it is expected that a Ps can create a new open space.<sup>18,25</sup> The bubble size is determined by a balance of forces between the Ps-molecule repulsion and the (microscopic) surface tension. It is, however, hard to understand why bubble formation should lead to smaller local free volumes than expected from the thermal expansion. From *PVT* experiments<sup>37</sup> it was found that the macroscopic volume shows a continued increase with  $T$ . We would expect similar behavior from the free volume also.

We assume, therefore, that, also at higher temperatures, *o*-Ps annihilates from (dynamic) holes in the amorphous structure. However, from the flattening of the hole volume vs.  $T$  dependence above  $180^\circ\text{C}$  we conclude that the behavior of the *o*-Ps lifetime  $\tau_3$  can no longer be attributed to a corresponding volumetric variation of the hole volume only. From mechanical and dielectrical relaxation experiments it is well known that with increasing temperature various motional and vibrational processes are stimulated in polymers with the tendency of increasing frequencies and amplitudes.<sup>38,39</sup> Localized motions such as rotation of side groups and around the main-chain bonds, local segmental mobility and cooperative relaxations of segments are discussed. EPR (electron paramagnetic resonance), NMR (nuclear magnetic resonance), and QENS (quasielastic neutron scattering) experiments deliver evidence that at higher temperatures processes with relaxation times well below 1 ns may occur.<sup>40,41</sup> In QENS experiments an E-process (elementary process) on a time scale from several tens to several hundreds of picoseconds was observed and attributed to local chain conformational transitions.<sup>41</sup>

As long as the relaxation times are significantly longer than the *o*-Ps lifetime of  $\tau_3 \sim 2$  ns, the polymer dynamics do not significantly change the size and shape of free-volume holes during the *o*-Ps life, i.e., the *o*-Ps pick-off lifetime mirrors the geometrical size of a local free volume at the “moment” of annihilation. Molecular motions with relaxation times smaller than  $\tau_3$ , however, cause a smearing in the molecule and electron density distribution during the *o*-Ps life, effectively raising the electron density in the free volume, or, in other words, decreasing the empty space inside a hole. This shortens  $\tau_3$  relative to its value in a “cold” polymer of the same mean hole size. Under favorable conditions the increase on heating of  $\tau_3$  with the free volume can be outweighed by the decrease caused by the thermal motion. For even stronger thermal motions we could imagine a decrease in the observed *o*-Ps lifetime. But now the Ps bubble effect, i.e., the Ps-molecule repulsion, might stabilize the local empty space sensed by the Ps probe.

From the  $v$  vs.  $T$  plot (Fig. 3) in the range  $60^\circ\text{C} < T < 180^\circ\text{C}$  we estimate a coefficient of thermal expansion of mean hole volume in the rubbery phase of  $\alpha_{h,r} = 5.7 \times 10^{-3} \text{ K}^{-1}$ . This is one order of magnitude larger than the expansion coefficient of the macroscopic volume in amorphous PA6<sup>42</sup>,  $\alpha_r = 6.0 \times 10^{-4} \text{ K}^{-1}$ . Unfortunately,  $\alpha_{h,g}$  cannot be estimated with sufficient accuracy from our current data. Typically,<sup>32,43</sup>  $\alpha_{h,g}$  is in the order of  $\approx 0.1 \alpha_{h,r}$ .

The coefficient of thermal expansion of the total volume,  $\alpha$ , may be related to that of the hole volume,  $\alpha_h$ , via

$$\alpha = \alpha_h h + \alpha_{\text{occ}}(h - 1) \quad (3)$$

In deriving relation eq. (3) we have assumed that the total volume  $V$  consists of the free volume  $V_f$  and the occupied (bulk or hypothetical equilibrium) volume  $V_{\text{occ}}$ ,  $V = V_f + V_{\text{occ}}$ , and that the free volume,  $V_f = N_h v$ , expands like the mean hole volume  $v$  without significant change in the number density of holes  $N_h$ .<sup>33,42,44–46</sup>  $h$  is the fractional free volume,  $h = V_f/V$ , and  $\alpha_{\text{occ}}$  denotes the coefficient of thermal expansion of the occupied volume. Applying this relation to both temperature regions  $T < T_g$  and  $T > T_g$ , and assuming that  $h$  behaves continuously at  $T_g$  and  $\alpha_{\text{occ}}$  does not change with  $T$ , allows to eliminate  $\alpha_{\text{occ}}$  and one obtains (for more details see references<sup>32,33,43</sup>)

$$h_g = (\alpha_r - \alpha_g)/(\alpha_{h,r} - \alpha_{h,g}). \quad (4)$$

Here  $h_g$  is the fractional free volume at the glass transition temperature,  $h_g = (V_f/V)_g$ ,  $(\alpha_r - \alpha_g)$  is the change of the (cubic) coefficient of thermal expansion of the macroscopic volume at  $T_g$  ( $\alpha_r = (1/V_r)dV/dT$ ,  $T > T_g$ , and  $\alpha_g = (1/V_g)dV/dT$ ,  $T < T_g$ ).  $(\alpha_{h,r} - \alpha_{h,g})$  denotes the same for the mean hole volume ( $\alpha_{h,r} = (1/v_r)dv/dT$ ,  $T > T_g$ , and  $\alpha_{h,g} = (1/v_g)dv/dT$ ,  $T < T_g$ ).

Values of  $\alpha_r = 6.0 \times 10^{-4} \text{ K}^{-1}$  and  $\alpha_g = 2.9 \times 10^{-4} \text{ K}^{-1}$  for PA6 can be found in the data collected by van Krevelen.<sup>42</sup> With these coefficients and  $\alpha_{h,r} - \alpha_{h,g} = 5.1 \times 10^{-3} \text{ K}^{-1}$  a fractional hole volume at  $T_g$  of  $h_g = 6.1\%$  follows. From this a number density of holes  $N_{hg} = h_g/v_g = 0.83 \text{ nm}^{-3}$  ( $v_g = 73 \text{ \AA}^3$ ) is calculated. This value correlates well with previous estimates of  $0.73 \text{ nm}^{-3}$  (polyethylene<sup>32</sup>),  $0.36 \text{ nm}^{-3}$  (polytetrafluoroethylene<sup>32</sup>), and  $\sim 1 \text{ nm}^{-3}$  [poly (diethylene glycol bis (allyl carbonate) networks<sup>44</sup>)],  $0.7 \text{ nm}^{-3}$  (ethylene–vinyl acetate copolymers<sup>47</sup>) and estimates for other polymers.<sup>45,46</sup> Assuming that the number of holes does not change with the temperature<sup>32,33,42,44–46</sup> the variation of the fractional free volume may be estimated from  $h(T) = N_{hg} [v(T) - v_g \alpha_{\text{occ}}(T - T_g)]$  (see the discussion in ref. 32).  $\alpha_{\text{occ}}$  may be approximated by  $\alpha_g = 2.9 \times 10^{-4} \text{ K}^{-1}$ . From our data we find that  $h$  changes from 5.8% at  $25^\circ\text{C}$  to 10.3% at  $220^\circ\text{C}$ .

### Humidity Sorption and Desorption during the Measurements in Laboratory Air

The parameters extracted for each PA6 specimen from the 2-h PALS spectra typically change between the first and the last, the 12, measurement performed at  $25^\circ\text{C}$  in laboratory air (Fig. 4). As mentioned previously, the specimens were equilibrated in atmospheres of fixed  $RH$  before starting these measurements. Typically, the *o*-Ps lifetime  $\tau_3$  decreases over time, while the *o*-Ps intensity  $I_3$  increases. The variations of the parameters are largest for high  $RH$ , small for  $0 < RH < 30\%$  and disappear almost for  $RH = 30–50\%$  (compare Fig. 3). We attribute the observed behavior to water desorption from the samples and water sorption into the samples during the measurement. Only those samples that are exposed to a humidity equal to that of the laboratory atmosphere ( $RH \approx 40\%$ ) are in a steady state condition during the measurement. An example is illustrated in Figure 4, which plots the *o*-Ps lifetime  $\tau_3$  and intensity  $I_3$  as a function of the square root of measurement time,  $t^{1/2}$ , for a sample saturated with moisture in an atmosphere of 100%  $RH$  and

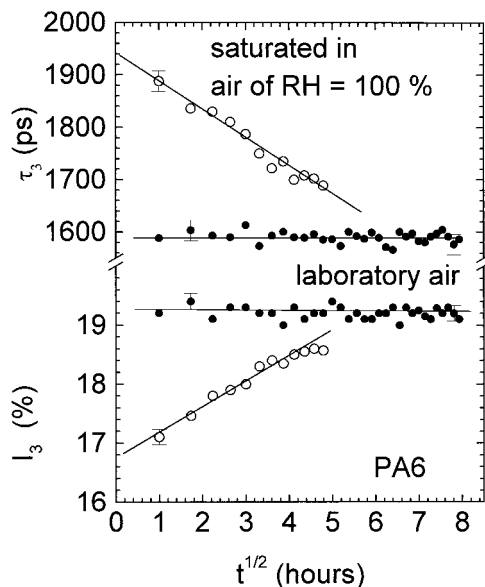


**Figure 4** Variation of  $\tau_3$  and  $I_3$  during the measurement in laboratory air. Empty symbols: the sample was equilibrated in an atmosphere of  $RH = 100\%$  before the measurement was started. Filled symbols: the sample was equilibrated in the laboratory atmosphere.

for another one equilibrated in the laboratory air. The *o*-Ps annihilation parameters vary approximately linearly with  $t^{1/2}$ . Such behavior we have detected already previously for a polyimide.<sup>48</sup> It is typically observed in sorption and desorption curves of mass uptake,<sup>49,50</sup> and serves as evidence for the validity of Fick's law of diffusion. PALS experiments show an enhanced sensitivity for surface-near regions in a sample, because the positron implantation profile follows a negative exponential,<sup>51</sup>  $\alpha \cdot \exp(-\alpha x)$  with  $\alpha = 42 \text{ cm}^{-1}$  for materials of mass density  $\rho \sim 1 \text{ g/cm}^3$ . The lifetime parameters of the specimen equilibrated in the laboratory air do not show any variation with time. This shows that no effects that could be attributed to the exposure of the PA6 sample to the irradiation from the positron source occur in the specimen. Frequently, a more or less strong variation of  $I_3$  with exposure time is observed.<sup>52</sup>

### The Influence of Humidity on the Local Free Volume

In Figure 3, the temperature dependent variation of the local free volume in the dry PA6,  $v_{\text{dry}}$ , is compared with changes of the hole volume at room temperature due to sorption of humidity,  $v_{\text{humid}}$ . The value of  $v_{\text{humid}}$  was calculated from eq. (2) using the  $\tau_3$  value obtained by extrapolating

the  $\tau_3$  vs.  $t^{1/2}$  behavior to  $t \rightarrow 0$  (compare Fig. 4). For comparison of  $v_{\text{humid}}$  with  $v_{\text{dry}}$ , the experimental data were plotted as a function of the difference between the temperature of measurements and the glass transition temperatures, i.e.,  $v_{\text{dry}}$  vs.  $[T - 54^\circ\text{C}]$  and  $v_{\text{humid}}$  vs.  $[25^\circ\text{C} - T_g(RH)]$  (bottom scale in Fig. 3). For estimation of  $T_g$  as function of the relative humidity  $RH$  we used the empirical relation

$$T_g(^{\circ}\text{C}) = a + b(\%RH) + c(\%RH)^{1/2}. \quad (5)$$

The constants  $a = 53.67$ ,  $b = -0.168$ , and  $c = -6.208$  were estimated by Khanna et al.<sup>9</sup> from dynamic (modulated) differential scanning calorimetric (DDSC) measurements of PA6 exposed to atmospheres of different  $RH$  in the range of 0 to 92%.  $T_g$  decreases from  $54^\circ\text{C}$  for  $RH = 0$  to  $-20^\circ\text{C}$  at  $RH = 92\%$ . This variation is similar to that estimated from the dynamic mechanical analysis (DMA) of moist PA6<sup>23</sup> (Ultramid B35W from BASF).

The relative water uptake  $\Delta m_w/m_p$  (taken from mass uptake of amorphous PA6 as a function of  $RH$ , plotted in Figure 1 of ref. 6), the number density of sorbed water molecules  $N_w$ , the  $T_g$  estimated from eq. (5), the *o*-Ps lifetime  $\tau_3$ , the corresponding hole volume  $v$  as well as the value  $\Delta v_g$  (see the next section) are shown in Table I as a function of  $RH$ . The number density of sorbed water molecules,  $N_w$ , was estimated from the mass uptake  $\Delta m_w/m_p$ . The mass of a water molecule is calculated from  $m_w = [18.02 \text{ g/mol}]/[6.02217 \times 10^{23} \text{ mol}^{-1}] = 3.0 \times 10^{-23} \text{ g}$ . Likewise, the volume of a water molecule (in the liquid phase) is given by  $v_w = [18 \text{ cm}^3/\text{mol}]/[6.02217 \times 10^{23} \text{ mol}^{-1}] = 30 \text{ \AA}^3$ . The number density of water molecules in the polymer-water mixture is calculated from

$$N_w = [(\Delta m_w/m_p)\rho_p]/m_w \quad (6)$$

where  $\rho_p = 1.08 \text{ g/cm}^3$  is the mass density of the amorphous PA6.<sup>42</sup> We assume that water molecules do not enter the crystalline regions of PA6.

The results in Figure 3 and Table I show that for small and medium  $RH$  the hole volume  $v_{\text{humid}}$  decreases first, followed by an increase above  $RH \approx 50\%$ . For higher  $RH$ ,  $v_{\text{humid}}$  exceeds the hole volume of the dry polymer at  $25^\circ\text{C}$  and approaches for  $RH \rightarrow 100\%$  the corresponding  $v_{\text{dry}}(T - T_g)$  values. This increase must be attributed mainly to the lowering of  $T_g$  to  $-25^\circ\text{C}$  for  $RH$

**Table I** The Relative Water Uptake  $\Delta m_w/m_p$  (Taken from Fig. 1 of Ref. 6), the Number Density of Sorbed Water Molecules  $N_w$  Estimated from Eq. (6), the  $T_g$  Estimated from eq. (5), the o-Ps Lifetime  $\tau_3$ , the Corresponding Hole Volume  $v$ , as Well as the Value  $\Delta v_g$  (See Text) as a Function of the Relative Humidity  $RH$

$RH$ (%)	$\Delta m_w/m_p$ (%)	$N_w$ (nm <sup>-3</sup> )	$T_g$ (°C)	$\tau_3$ (ps)	$v$ (Å <sup>3</sup> )	$\Delta v_g$ (Å <sup>3</sup> )
0	0.00	0.00	54	1693	70.0	0
11	1.60	0.58	31	1641	65.0	-9.5
32	2.65	0.95	13	1595	61.7	-16.0
45	3.20	1.15	4	1610	62.9	-19.4
55	4.15	1.49	-2	1650	66.0	-18.5
75	5.90	2.12	-13	1707	71.1	-17.7
90	8.40	3.02	-20	1801	79.2	-12.9
100	10.00	3.60	-25	1942	92.1	-1.90

= 100%.<sup>9</sup> At  $T = 25^\circ\text{C}$  the humid ( $RH > 50\%$ ) PA6 is in the rubbery phase. In this phase the slope of  $v(T)$  is large, which leads to the observed increase in the hole volume with decreasing  $T - T_g$ . However, this effect alone cannot explain the observed behavior of the hole volume  $v$  calculated from  $\tau_3$ .

To understand the variation of  $v$  as a function of  $RH$  we have to consider the change in  $T_g$  as well as a possible change in the mean hole size at  $T_g$ ,  $v_g$ , due to water sorption. In the following section we present a phenomenological model that follows the philosophy of previous works<sup>12–15</sup> on the behavior of the specific volume. We assume that the  $v(T)$  curve can be approximated by two straight lines of different slopes:

$$v(T) = v_g + e_{ph,g}(T - T_g) \text{ for } T < T_g \quad (7)$$

$$v(T) = v_g + e_{ph,r}(T - T_g) \text{ for } T > T_g \quad (8)$$

$e_{ph,g} = [dv_p/dT]_{T < T_{pg}}$  and  $e_{ph,r} = [dv_p/dT]_{T > T_{pg}}$  denote the expansivity of  $v_p(T)$  in the glassy and rubbery state of the polymer. For simplicity, we assume further that  $e_{ph,g}$  and  $e_{ph,r}$  do not change with  $RH$  (at least within the range  $\Delta m_w/m_p \leq 10\%$  of water uptake). This assumption seems to be justified, considering the thermal expansion coefficients of the specific volume of polymer-diluent mixtures published by Kinjo and Nakagawa.<sup>53</sup> We allow, however,  $T_g$  and  $v_g$  to vary as a consequence of water uptake. The variation of  $T_g$  in PA6 as a function of  $RH$  is known from eq. (5). Thus, we have to analyze the variation of  $v_g$  to explain the observed behavior of  $v$ . If the shift in  $T_g$  was the only effect caused by the water sorption (without any change in  $v_g$ !), both curves plot-

ted in Figure 3 vs.  $T - T_g$  should agree. This is clearly not the case. The difference  $\Delta v(T - T_g) = v_{humid}(25^\circ - T_g(RH)) - v_{dry}(T - 54^\circ\text{C})$ , which is plotted in the subfigure of Figure 3 and in Figure 5, corresponds within our model to just the difference in the  $v_g$  of the humid and dry polymer,  $\Delta v = \Delta v_g = v_{humid,g} - v_{dry,g}$ .

The plots in Figure 6 should demonstrate the proposed model for the local free volume behavior in polymer–water mixtures more in detail.  $v_p(T)$  (solid lines) describes the temperature dependence of the hole volume in the pure (dry) polymer,  $T_{pg}$  and  $v_{pg}$  are its glass transition temper-

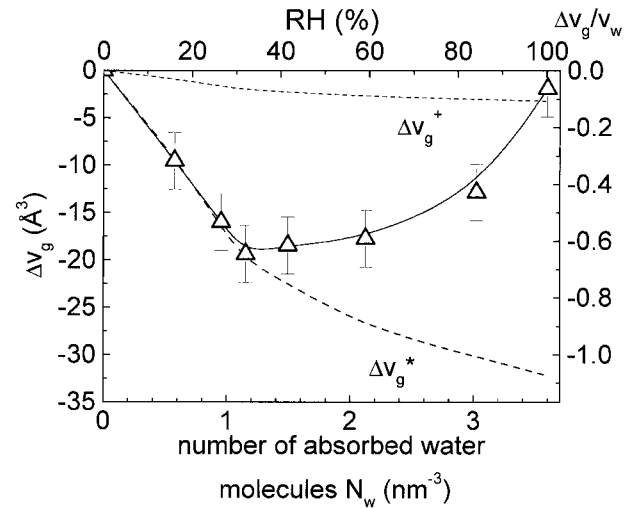


**Figure 5**  $\Delta v_g = v_{humid,g} - v_{dry,g}$ , as in the subfigure of Figure 3, in Å<sup>3</sup> and in units of the volume of a water molecule,  $\Delta v_g/v_w$ , but as a function of the relative humidity  $RH$  and the corresponding number of absorbed water molecules,  $N_w$ .



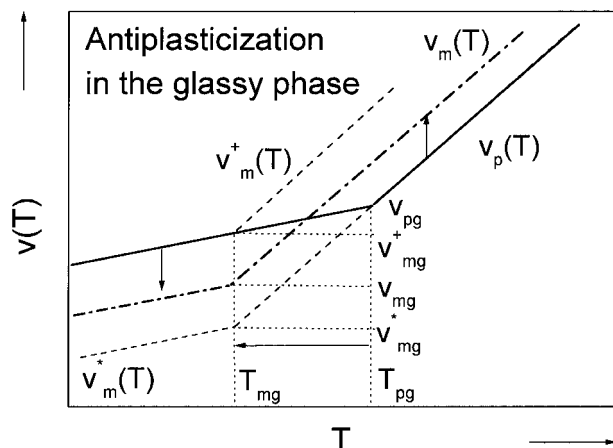


**Figure 6** A schematic diagram of the volumetric behavior of the free-volume holes in a mixture of a polymer with a diluent,  $v_m$ , exhibiting antiplasticization (i.e., a loss of free volume) in the glassy phase.  $v_p$  (solid line) denotes the pure polymer,  $v_m^*$  and  $v_m^+$  (dashed lines) are the hole volumes for maximum and no antiplasticization (see the text).

ature and the hole volume at  $T_{pg}$ .  $v_m(T)$ ,  $T_{mg}$ , and  $v_{mg}$  denote the corresponding values for the water–polymer mixture.

Typical low molecular weight diluents have a larger specific volume that the high molecular weight polymer has, but a lower glass transition temperature. The free volume of the polymer is influenced in two ways by adding a diluent. When initially added above  $T_g$  the diluent typically increases the free volume of the polymer–diluent mixture compared with the pure polymer, because more free volume is associated with the diluent than the polymer. From results in the literature,<sup>54,55</sup> we expect that this is also true for the mean size of holes forming the free volume. The overall specific volume of the system increases also. However, as the polymer–diluent system is cooled, a lower temperature must be attained before the mixture enters the glassy state. Clearly, there are two opposing influences on the volumetric behavior of a polymer system associated with the addition of a diluent. If the second influence dominates, the corresponding specific volume of the resulting polymer–diluent mixture deviates from the rule of additivity and the free volume can be smaller than that in the pure glassy polymer. This volumetric behavior may be described as antiplasticization, it is illustrated in Figure 6 by the curve  $v_m(T)$ .

Maximum loss of free volume, i.e., antiplasticization, in the glassy state of the mixture (without

loss of free volume in the rubbery state in the temperature range  $T > T_{pg}$ ) occurs when the first influence disappears. This is illustrated in Figure 6 by the curve  $v_m^*(T)$ . For  $T > T_{pg}$ , the difference  $v_m^*(T) - v_p(T)$  is zero. In range  $T < T_{mg}$ , the difference is given by  $v_m^*(T) - v_p(T) = v_{mg}^* - v_{pg}$  with

$$v_{mg}^* - v_{pg} = e_{ph,r}(T_{mg} - T_{pg}). \quad (9)$$

Because  $T_{mg} < T_{pg}$ ,  $v_{mg}^* - v_{pg} < 0$  follows. The antiplasticization of the glassy mixture disappears for

$$v_{mg}^+ - v_{pg} = e_{ph,g}(T_{mg} - T_{pg}). \quad (10)$$

In this case,  $v_m^+(T) - v_p(T) = 0$  for  $T < T_{mg}$  and  $v_m^+(T) - v_p(T) > 0$  for  $T > T_{pg}$ , i.e., a gain of free volume (plasticization) occurs in the rubbery but, as assumed, not in the glassy phase of the mixture. The curve  $v_m(T)$  in Figure 6 describes the general case of antiplasticization in the glassy phase. It occurs when the difference between the hole volume of the polymer–diluent mixture and the pure polymer at the glass transition is in the range

$$e_{ph,g} \leq (v_{mg} - v_{pg}) / (T_{mg} - T_{pg}) \leq e_{ph,r}. \quad (11)$$

As can be observed in Figure 6, there is a limited temperature range,  $T_{mg} < T < T_c < T_{pg}$  in which antiplasticization, i.e.,  $v_m(T) < v_p(T)$ , occurs in the rubbery state of the mixture. The smaller  $v_{mg}(T)$ , the larger is this range. The first influence discussed previously dominates the volumetric behavior if the amount of the difference  $v_{mg} - v_{pg}$  is smaller than given by eq. (10). In this case, plasticization can be observed in both the rubbery and also the glassy phase.

In the subfigure of Figure 3 and in Figure 5 we have plotted the values of  $\Delta v = \Delta v_g = v_{mg} - v_{pg}$  from the experiment together with the corresponding values from our model for maximum ( $\Delta^* v_g$ ) and no ( $\Delta^+ v_g$ ) loss of free volume (antiplasticization) in the glassy phase. As can be observed, in the first stage of water sorption into PA6 the values of  $\Delta v_g$  closely follow the curve for maximum loss of free volume.  $v_g$  has its largest decrease of  $19 \text{ \AA}^3$  for  $RH = 45\%$ ,  $T - T_g = -20^\circ\text{C}$ , and  $\Delta m_w/m_p = 3.2\%$ . From the mass uptake a number density of sorbed water molecules of  $N_w = 1.2 \text{ nm}^{-3}$  follows. This value is larger but in the same order of magnitude than the number of free-

volume holes,  $N_h = 0.8 \text{ nm}^{-3}$ . The maximum decrease of the mean hole volume at  $T_g$ ,  $\Delta v_g$ , is equivalent to somewhat more than half of the volume of a water molecule in liquid water,  $\Delta v_g/v_w = 19 \text{ \AA}^3/30 \text{ \AA}^3 = 0.63$ . Assuming a simple hole filling model<sup>48,56</sup> and a complete occupation of all holes by a water molecule, a partial molecular volume of water absorbed by PA6 of  $(1 - 0.63)v_w = 0.37v_w = 11 \text{ \AA}^3$  for  $RH = 45\%$  would follow from this value. From investigations of the volume expansion during water absorption of a (glassy) polyimide, we estimated previously<sup>48</sup> a partial molecular volume of  $16 \text{ \AA}^3$  for a water uptake of  $\Delta m_w/m_p = 1.5\%$ .

The observed lowering of local free volume correlates sufficiently well to the behavior of the specific volume of PA6 due to water sorption, which for small and medium  $RH$  exhibits smaller values than expected from the rule of additivity.<sup>22</sup> For PA66, which behaves similar to PA6, more accurate data are available. The partial specific volume of water increases from  $0.5 \text{ cm}^3/\text{g}$  for the first water molecules absorbed to  $0.85 \text{ cm}^3/\text{g}$  for a water uptake in the range of 2 to 5 mass-%.<sup>3-5</sup>

The number density of water molecules for  $RH = 55\%$  corresponds approximately to a concentration of one water molecule per two amide groups. As previously mentioned, Puffr and Sebenda<sup>3</sup> considered that this level, which probably corresponds to water molecules hydrogen bound to the oxygen atoms of two amide groups, represents the first and most strongly bound type of absorbed water. Our conclusion of almost maximum antiplasticization (indicated as decrease in the mean local free volume) of PA6 may correlate with this hypothesis. The displacement of the amide–amide bonds associated with highly strained chain conformations may improve the packing resulting in the decrease of  $v_g$ . Unfortunately, we cannot determine from our experiments whether the observed decrease in the mean local free volume at  $T_g$  is due to this effect, or simply due to the filling of the preexisting free volume holes with water molecules. Probably, both models do not contradict each other.

For  $RH$  larger than 55%,  $v_g$  (and, therefore, also  $\Delta v_g$ ) increases distinctly and approaches the values for disappearing antiplasticization (or possibly appearing plasticization) in the glassy phase of the polymer–water mixture. This observation correlates well with the known increase of the partial specific volume of water in polyamides from  $0.85$  to  $1\text{--}1.2 \text{ cm}^3/\text{g}$  for  $RH$  larger than 90%.<sup>4,5</sup> Obviously, for high  $RH$  the water to be

absorbed is packed much less favorably than that absorbed earlier.

From the curvature in the absorption isotherm in the range  $RH > 60\%$  it was concluded that the water forms clusters containing two and, near 100% humidity, three water molecules per cluster.<sup>3-6</sup> This estimation corresponds Puffr and Sebenda's second stage of water absorption, which is three molecules per two amide groups in the amorphous regions. The second and third water molecules were said to be loosely bound between the carbonyl of one amide group and the NH of another.<sup>3</sup> The incorporation of this loosely bound water weakens the already existing H bonds and leads to plasticization. This plasticization effect compensates more and more the antiplasticization of the polymer due to the firmly bound water and nullifies it finally. It leads also to the further decrease of  $T_g$ .

The behavior of the free-volume hole size as function of the glass transition temperature, observed in Figure 3, seems to be typical for polymer–diluent mixtures. In glassy polymers such as polyimides the mean hole volume  $v$  decreases during sorption of moisture,<sup>48</sup> organic vapor,<sup>54</sup> or  $\text{CO}_2$  gas.<sup>55</sup> This behavior was interpreted in terms of the Langmuir-type sorption. The sorbed molecules were assumed to occupy first larger holes of a size distribution of preexisting saturable holes resulting in a decrease of the mean size of unoccupied holes.<sup>48,56</sup> For rubbery polymers, such as polyethylene, however, the local free volume increases during sorption of organic vapor or  $\text{CO}_2$ , which is attributed to the Henry-type sorption.<sup>54,55</sup> The sorbed molecules dissolve into the chains and participate in the micro-Brownian motions. As a result, the hole size distribution broadens, and shifts to higher mean sizes. Similar volumetric behavior as in our experiments was recently observed by Ito et al.<sup>55</sup> and Bohlen et al.<sup>56</sup> These authors detected a decrease in the hole size in polycarbonate (PC) during sorption of  $\text{CO}_2$  gas for low gas pressures. This decrease was analyzed in terms of the hole filling model.<sup>56</sup> For pressures higher than 0.5 MPa the hole size increased, which was attributed to swelling due to the high concentration of gas molecules.

## CONCLUSION

In dry PA6 plates the mean free-volume hole size varies between  $r = 2.55 \text{ \AA}$ ,  $v = 70 \text{ \AA}^3$  and  $r = 3.17 \text{ \AA}$ ,  $v = 128 \text{ \AA}^3$  when the temperature increases

from 25 to 220°C. From the comparison of the coefficients of the thermal expansion of specific (macroscopic) and local free volume a number density of holes  $N_h$  of  $0.8 \text{ nm}^{-3}$  was estimated.

The exposure of PA6 to humidity results in a decrease in the local free volume  $v$ , detected at 25°C, up to a  $RH$  of 40% followed by an increase for  $RH > 50\%$ . This behavior was discussed on the basis of a phenomenological model in which the glass transition temperature  $T_g$  and the mean local free volume at  $T_g$ ,  $v_g$ , of the moist polyamide were allowed to vary with  $RH$ . In the range  $0 < RH < 90\%$ ,  $v_g$  was always smaller than in the dry PA6. This decrease in the local free volume of the water-polymer mixture with respect to that of the pure glassy polymer can be considered as the reason of the well known negative departure of the specific volume from the ideal volume additivity.

Two stages of sorption behavior were observed. For small and medium  $RH$ , the polymer-water mixture shows maximum loss of free volume (antiplasticization):  $v_g$  drops down by up to  $19 \text{ \AA}^3$  for  $RH = 45\%$ , which is more than half of the volume of a water molecule. This observation can be discussed in terms of filling of preexisting free volume holes by water molecules. It was, however, also considered as being in agreement with the hypothesis of Puffr and Sebenda<sup>3</sup> on the existence of firmly bound water molecules. These are believed to displace the amide-amide bonds associated with highly strained chain conformations, which may improve the packing.

For  $RH > 50\%$ ,  $v_g$  increases again and approach for  $RH \approx 100\%$  the value (in the scale  $T - T_g$ ) of the corresponding dry PA6. This observation appears in agreement with the hypothesis of water molecules loosely bound the carbonyl of one amide group and the NH of another.<sup>3</sup> The incorporation of this loosely bound water weakens the already existing H bonds and leads to plasticization. This plasticization effect compensates more and more the antiplasticization due to the firmly bound water and finally nullifies it.

The authors wish to thank D. Bamford (Bristol) for critical reading of the manuscript.

## REFERENCES

1. For example, see Goldstein, M.; Simha, R. *The Glass Transition and the Nature of the Glassy State*; New York Academy of Science: New York, 1976; Allen, G.; Petrie, S. E. B. (Eds.), *Physical Structure of the Amorphous State*; Marcel Dekker: New York 1976; Perez, J. *Physics and Mechanics of Amorphous Polymers*; Balkema, A. A., Eds.; Brookfield: Rotterdam, 1998.
2. Rowland, St. P., Ed. *Water in Polymers*; ACS Symp Series 127; American Chemical Society: Washington, DC, 1980.
3. Puffr, R.; Sebenda, J. *J Polym Sci C* 1967, 16, 79.
4. Starkweather, H. W., Jr., in ref. 2, p. 433.
5. Starkweather, H. W., Jr.; Barkley, J. R. *J Polym Sci Polym Phys Ed* 1981, 19, 1211.
6. Frank, B.; Frübing, P.; Pissis, P. *J Polym Sci B Polym Phys* 1996, 34, 1853.
7. Laredo, E.; Jernandez, M. C. *J Polym Sci B Polym Phys* 1997, 35, 2879.
8. Pathmanathan, K.; Cavaille, J. Y.; Johari, G. P. *J Polym Sci B Polym Phys* 1992, 30, 341.
9. Khanna, Y. P.; Kuhn, W. P.; Sichina, W. J. *Macromolecules* 1995, 28, 2644.
10. Fujita, H. *Fortschr Hochpolym Forsch* 1961, 3, 1.
11. Vrentas, J. S.; Duda, J. L. *J Polym Sci B* 1977, 15, 403.
12. Vrentas, J. S.; Duda, J. L.; Ling, H.-C. *Macromolecules* 1988, 21, 1470.
13. Ruiz-Trevino, F. A.; Paul, D. R. *J Polym Sci B Polym Phys* 1998, 36, 1037.
14. Duda, J. L.; Romdhane, I. H.; Danner, R. P. *J Non-Cryst Solids* 1994, 172-174, 715.
15. Vrentas, J. S.; Vrentas, C. M. *J Polym Sci B Polym Phys* 1992, 30, 1005.
16. Eldrup, M.; Lightbody, D.; Sherwood, J. N. *Chem Phys* 1981, 63, 51.
17. Nakanishi, H.; Jean, Y. C. in *Positron and Positronium Chemistry, Studies in Physical and Theoretical Chemistry*; Schrader, D. M.; Jean, Y. C., Eds.; Elsevier Sci. Publ.: Amsterdam, 1988, p. 159, vol. 57.
18. Jean, Y. C. *Microchem J* 1990, 42, 72; and in *Positron Annihilation, Proc. 10th Int. Conf.*; He, Y. J.; Cao, B.-S.; Jean, Y. C., Eds.; *Mater Sci Forum Trans Tech Publ* 1995, 175-178, 59.
19. Pethrick, R. A. *Prog Polym Sci* 1997, 22, 1.
20. Jean, Y. C.; Eldrup, M.; Schrader, D. M.; West, R. N., Eds.; *Positron Annihilation, Proc. of the 11th Int. Conf.*, Kansas City, MO, May 1997; *Mater Sci Forum* 1998, 255-257; Triftshäuser, W.; Kögel, G.; Sperr, P., Eds.; *Positron Annihilation, Proc. of the 12th Int. Conf.*, ICPA-12, München, August 6-12, 2000, *Materials Science Forum*; *Trans. Techn. Publications: Uetikon-Zuerich, Switzerland*, 2001, vol. 363-365; Ito, Y.; Suzuki, T.; Kobayashi, Y., Eds. *Radiat Phys Chem* 2000, 58, 401.
21. Chuang, S. Y.; Tao, J.; Wilkenfeld, J. M. *J Appl Phys* 1972, 43, 737.
22. Singh, J. J.; St. Clair, T. L.; Holt, W. H.; Mock, W., Jr. *Nucl Instr Methods* 1984, 221, 427.

23. Welande, M.; Maurer, F. H. *Mater Sci Forum* 1992, 105–110, 1815.
24. Dlubek, G.; Stolp, M.; Nagel, Ch.; Fretwell, H. M.; Alam, M. A.; Radusch, H.-J. *J Phys Condens Matter* 1998, 10, 10443.
25. Mogensen, O. E. *Positron Annihilation in Chemistry*; Springer-Verlag: Heidelberg, 1995.
26. Franke, H.; Wagner, D.; Kleckers, T. *Appl Optics* 1993, 32, 2927.
27. Greenspan, L. *J Res Nat Bur Stand A* 1977, 81, 89.
28. LIFSPECFIT 5.1, Lifetime Spectrum Fit Version 5.1; Technical University of Helsinki: Laboratory of Physics, 1992.
29. Shukla, A.; Peter, M.; Hoffmann, L. *Nucl Instr Methods A* 1993, 335, 310; Hoffmann, L.; Shukla, A.; Peter, M.; Barbiellini, B.; Manuel, A. A. *Nucl Instr Methods A* 1993, 335, 276.
30. Nakanishi, H.; Jean, Y. C.; Smith, E. G.; Sandreczki, T. C. *J Polym Sci B Polym Phys* 1989, 27, 1419.
31. Nakanishi, H.; Jean, Y. C. *Macromolecules* 1991, 24, 6618.
32. Dlubek, G.; Saarinen, K.; Fretwell, H. M. *J Polym Sci B Polym Phys* 1998, 36, 1513.
33. Dlubek, G.; Alam, M. A.; Saarinen, K.; Stejny, J.; Fretwell, H. M. *Acta Phys Polonia* 1999, 95, 521.
34. Dlubek, G.; Hübner, Ch.; Eichler, S. *Nucl Instr Methods B* 1998, 142, 191; Dlubek, G.; Eichler, S.; Hübner, S.; Nagel, Ch. *Nucl Instr Methods B* 1999, 149, 501; Dlubek, G.; Eichler, S.; Hübner, Ch.; Nagel, Ch. *Phys Stat Sol (a)* 1998, 168 333; 1999, 172, 303; 1999, 174, 313.
35. Deng, Q.; Sundar, C. S.; Yean, Y. C. *J Phys Chem* 1992, 96, 492.
36. Brandt, W.; Spirn, J. *Phys Rev* 1966, 142, 231.
37. Owell, R. A. in *Physical Properties of Polymers Handbook*; Mark, J. E., Ed.; AIP Press: Woodbury, NY, 1996.
38. Matsuoka, S. *Relaxation Phenomena in Polymers*; Hanser Publ.: Munich, 1992.
39. Donth, E.-J. *Relaxation and Thermodynamics in Polymers, Glass Transition*; Akademie Verlag: Berlin, 1992.
40. Kim, S. S.; Yavrouian, A. H.; Liang, R. H. *J Polym Sci B Polym Phys* 1993, 31, 495.
41. Kanaya, T.; Kawaguchi, T.; Kahi, K. *Macromolecules* 1999, 32, 1672.
42. Van Krevelen, D. W. *Properties of Polymers*; Elsevier Sci. Publ. Co.: Amsterdam, 1990.
43. Hristov, H. A.; Bolan, B.; Ye, A. F.; Xie, L.; Gidley, D. W. *Macromolecules* 1996, 29, 8507.
44. Dlubek, G.; Stejny, J.; Alam, M. A. *Macromolecules* 1998, 31, 4574.
45. Schmidt, M.; Maurer, F. H. *Macromolecules* 2000, 33, 3879; Maurer, F. H.; Schmidt, M. *Radiat Phys Chem* 2000, 58, 509.
46. Srithawatpong, R.; Peng, Z. L.; Olson, B. G.; Jamieson, A. M.; Simha, R.; McGervey, R. J. D.; Maier, T. R.; Halasa, A. F.; Ishida, H. *J Polym Sci B Polym Phys* 1999, 37, 2754.
47. Dlubek, G.; Lüpke, Th.; Stejny, J.; Alam, M. A.; Arnold, M. *Macromolecules* 2000, 33, 990.
48. Dlubek, G.; Buchhold, R.; Hübner, Ch.; Nakladal, A. *Macromolecules* 1999, 32, 4574.
49. Lim, B. S.; Nowick, A. S.; Lee, K.-W.; Viehbeck, A. *J Polym Sci B Polym Phys* 1993, 31, 545.
50. Barrie, J. A. In *Diffusion in Polymers*; Crank, J.; Park, G.S., Eds.; Academic Press: London, 1968.
51. Dupasquier, A.; Mills, A. T. Jr., Eds. *Positron Spectroscopy of Solids, Proc. Int. School "Enrico Fermi," Varenna, Italy, July 1993*, IOS Press: Amsterdam, 1995.
52. Hirade, T.; Maurer, F. H. J.; Eldrup, M. *Radiat Phys Chem* 1993, 58, 465.
53. Kinjo, N.; Nakagawa, T. *Polym J* 1973, 4, 143.
54. Ito, Y.; Sanchez, V.; Lopez, R.; Fucugauchi, L. A.; Tanaka, K.; Okamoto, K. *Bull Chem Soc Jpn* 1993, 66, 727.
55. Ito, Y.; Mohamed, H. F. M.; Tanaka, K.; Okamoto, K.; Lee, K. H. *J Radioanal Nucl Chem* 1996, 211, 211.
56. Bohlen, J.; Wolff, J.; Kirchheim, R. *Macromolecules* 1999, 32, 3766.